

General Dispersion Relation for Electromagnetic Surface Waves in Partially-Filled Cylindrical Plasma Waveguides with Finite Wall Conductivity

Wafa. M. Daqa^{1*}

¹Physics Department, King Faisal University (till 16/9/2025), Hufuf, Saudi Arabia.

*Corresponding author: E-mail: wafamahmood23@gmail.com

ABSTRACT

In the absence of an external magnetic field, surface plasma waves can travel over the plasma-vacuum interface in a cold homogenous plasma encased in a cylindrical metallic waveguide as long as the plasma only partially fills the waveguide. In this work, we examine the impact of the metallic wall's finite conductivity on the dispersion relation of surface plasma waves. We obtain a general dispersion relation for any azimuthal harmonic number by starting with Maxwell's equations and using the field-matching approach. The analysis and numerical computations are then concentrated on the electrostatic dipolar mode. The dispersion relation is investigated for a range of wall conductivities and waveguide radius to plasma radius ratios. Additionally, our results match well with earlier research and are compatible with the limiting scenario of perfectly conducting walls. Understanding wave dynamics is essential for beam diagnostics and wakefield studies in plasma-based antennas, waveguide design, and accelerator physics research. This work offers fresh perspectives on electromagnetic wave propagation in practical plasma waveguides.

Keywords: Cold Homogenous Plasma, Dispersion Relation, Dipole Mode, Surface Plasma Waves, Resistive Cylindrical Pipe.

1. INTRODUCTION

Surface plasma waves (SPW) are bounded plasma modes, where their propagation is possible due to the dependence of the plasma permittivity on frequency that becomes negative for frequencies below the plasma frequency. When plasma is bounded by a dielectric of positive permittivity, surface waves can propagate along the boundary with exponential-like decay fields away from the boundary (Landau & Lifshitz, 1960; Aliev et al., 2000).

There are various applications of the SPW supported by both gaseous and solid-state plasma waveguide systems due to their localization and resonant features. The fields of the traveling SPW can be provided to sustain a plasma, and such a "guided-wave-produced plasma" has some advantages over the DC discharge plasma since it is electrode-less (Aliev et al., 2000; Moisan & Zakrzewski, 1991). These plasma sources are used for various applications such as surface treatment, light sources for spectroscopy, laser physics (Moisan et al., 1982; Kumar et al., 2023; Varma et al., 2023; Varma et al., 2024). Plasma waveguides have wide applications in microwave and millimeter technology (Polo Jr & Lakhtakia, 2011). They can serve as antennas for wireless communication systems (Grewal & Hanson, 2003), and they can be utilized in refractive index sensing technology (Sital & Sharma, 2017; Chen et al., 2018; Ruan et al., 2018). Furthermore, plasma waveguides

can provide a well confined adjustable region that are capable of supporting and manipulating high currents beams. Therefore, they have applications in accelerator physics (Liu, 2007). Considering surface waves modes in studying beam instability and impedance calculation can enhance the accuracy of modeling beam dynamics (Al-Khateeb et al., 2008).

Studying the eigenmodes of such plasma waveguides is important for their operation and development. Theoretically, such study is performed by finding the dispersion relation for an assumed mathematical model of the plasma. The excitation of surface waves in a homogenous cold plasma was first investigated by Trivelpiece and Gould as a diagnostic method for measuring that plasma's electron density (Trivelpiece, 1958; Trivelpiece & Gould, 1959). They found that when a plasma is of finite transverse cross section, space charge waves may propagate even in the absence of a drift motion or thermal velocities of the plasma particles. In their pioneering experimental investigation of surface plasma waves, they used a cylindrical plasma column enclosed in a glass tube that was coaxial with a perfect conducting circular metallic waveguide. They employed the electrostatic theory to derive the dispersion relation for any harmonic number. Y. Akao et al. considered the retardation effects for the same geometry without the metallic pipe (Akao & Ida, 1964).

In general, when the pipe wall is not perfectly conducting, the electromagnetic fields are mixture of transverse electric (TE) and transverse magnetic (TM). The only exception is the case of the axially symmetric monopole corresponding to the azimuthal harmonic number $m=0$ in axially symmetric pipe. The spectra of electromagnetic surface waves on plasma-vacuum interface inside a metallic resistive pipe was studied by W. M. Daqa et al. only for the azimuthally symmetric mode (Daqa et al., 2008).

In this work we adopt the same geometry and the properties of materials of all regions as in (Daqa et al., 2008) but we assume there is an azimuthal dependence, then we derive a more general dispersion relation for any azimuthal harmonic number m . We focus the analysis on the dipolar mode; $m=1$. In section 2 we give the analytical derivation of the general dispersion, and we took certain approximations to validate our formula. Finally, in section 3 we perform a numerical analysis for the dipolar mode to see the effect of the wall's resistivity and the ratio of wall radius to plasma radius on the dispersion relation. The results of the recent work can be used in plasma-based slow-wave structures, impedance modeling for accelerators, and plasma coating for electromagnetic shielding.

1.1. Derivation of the General Dispersion Relation

Consider the plasma waveguide structure that is shown in figure 1. It consists of a plasma column of radius a concentric with a resistive thick pipe of radius b such that $b > a$. The plasma is assumed to be isotropic, cold, collision-less, and unmagnetized. Hence, the plasma dielectric function is given by $\epsilon_p = 1 - \omega_p^2/\omega^2$.

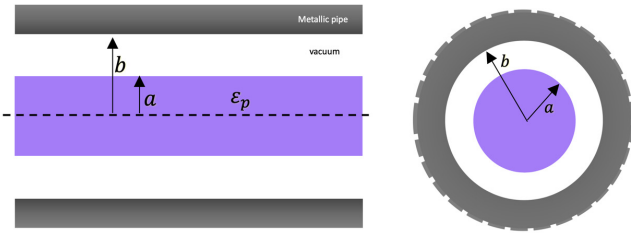


Fig. 1 The metallic waveguide structure with internal radius b that is filled partially with plasma of radius a .

Assume that the spatial and temporal dependence of the electromagnetic (em) fields follows the form $f_m(r) \exp(i(m\phi + kz - \omega t))$, where $m=0,1,2,\dots$ is the field's azimuthal variations number. Substituting that form for \vec{E}_m and \vec{B}_m in the Maxwell's curl equations, we obtain six equations in terms of fields components. Then solving these equations for the transverse electromagnetic field components in terms of the longitudinal fields E_{zm} and B_{zm} results in

the following,

$$E_{rm}(r) = \frac{-i}{\tau_i^2} \left(k \frac{dE_{zm}}{dr} + \frac{im\omega}{r} B_{zm} \right) \quad (1)$$

$$E_{\phi m}(r) = \frac{-i}{\tau_i^2} \left(\frac{imk}{r} E_{zm} - \omega \frac{dB_{zm}}{dr} \right) \quad (2)$$

$$B_{rm}(r) = \frac{i}{\tau_i^2} \left(\frac{im\omega\mu_0\epsilon_i}{r} E_{zm} - k \frac{dB_{zm}}{dr} \right) \quad (3)$$

$$B_{\phi m}(r) = \frac{-i}{\tau_i^2} \left(\omega\mu_0\epsilon_i \frac{dE_{zm}}{dr} + \frac{imk}{r} B_{zm} \right) \quad (4)$$

with the radial propagation constant τ_i and the permittivity ϵ_i in each region,

$$\begin{aligned} \tau_p^2 &= k^2 - \frac{\omega^2}{c^2} \epsilon_p, \quad \epsilon_p = \epsilon_0 \epsilon_p, \quad \text{for plasma} \\ \tau_v^2 &= k^2 - \frac{\omega^2}{c^2}, \quad \epsilon_v = \epsilon_0 \quad \text{for vacuum} \end{aligned} \quad (5)$$

The wave equations for E_{zm} and B_{zm} are given by,

$$r \frac{d}{dr} \left(r \frac{dE_{zm}}{dr} \right) - (m^2 - (\tau_i r)^2) E_{zm} = 0 \quad (6)$$

$$r \frac{d}{dr} \left(r \frac{dB_{zm}}{dr} \right) - (m^2 - (\tau_i r)^2) B_{zm} = 0 \quad (7)$$

The general solutions of (6) and (7) are expressed in terms of the modified Bessel's functions of order m , namely,

$$E_{zm} = \begin{cases} A_1 I_m(\tau_p r) & 0 \leq r \leq a \\ A_2 I_m(\tau_v r) + A_3 K_m(\tau_v r) & a \leq r \leq b \end{cases} \quad (8)$$

$$B_{zm} = \begin{cases} B_1 I_m(\tau_p r) & 0 \leq r \leq a \\ B_2 I_m(\tau_v r) + B_3 K_m(\tau_v r) & a \leq r \leq b \end{cases} \quad (9)$$

We find all integration's constants in (8) and (9) by applying the appropriate boundary conditions. The first set of boundary equations results from the continuity of the tangential components of em fields,

$$\hat{n} \times \vec{E} |_{r=a} = 0, \quad \hat{n} \times \vec{B} |_{r=a} = 0 \quad (10)$$

At the good conducting inner wall of the pipe, i.e., at $r=b$, we apply the impedance or Leontovetch boundary condition (Leontovich, 1948; Zotter & Kheifets, 1998),

$$\vec{E} = \hat{n} \times \frac{Z_s}{\mu_0} \vec{B} |_{r=b}, \quad Z_s = \sqrt{\frac{\mu_0 \omega}{2 \sigma_c}} (1 - i) \quad (11)$$

where Z_s is the surface impedance of the metallic pipe, and σ_c its conductivity.

By imposing the boundary conditions in (10) and (11), on the general solutions in (8) and (9), we obtain the dispersion relation for any azimuthal mode of order m propagates in a resistive pipe that is partially filled with cold unmagnetized plasma as follows,

$$\begin{aligned} \omega^2 \mu_0 \epsilon_0 \epsilon_p \tau_p^2 I_m^2(\tau_p a) \chi_{11} \chi_{22} \\ + \frac{m^2 k^2}{a^2} I_m^2(\tau_p a) \chi_{12} \chi_{21} = 0 \end{aligned} \quad (12)$$

where,

$$\chi_{11} = a_{11} + a_{12} \quad , \quad \chi_{22} = b_{21} + b_{22}, \quad (13)$$

$$\chi_{12} = b_{11} + b_{12} \quad , \quad \chi_{21} = a_{21} + a_{22} \quad (14)$$

Since the surface waves propagate slower than the speed of light, so we can use the quasi-static approximation; $\tau_p = \tau_v = k$ [Daqa et al., 2008]. As a result, the dispersion relation (12) becomes,

$$\omega^2 \mu_0 \epsilon_0 \epsilon_p I_m'^2(ka) b_{22}(a_{11} + a_{12}) + \frac{m^2}{a^2} I_m^2(ka) a_{22}(b_{11} + b_{12}) = 0 \quad (15)$$

where,

$$a_{11} = 1 - \frac{K_m(ka)}{I_m(ka)} f_1 - \frac{1}{\epsilon_p} \left(1 - \frac{K_m'(ka)}{I_m'(ka)} f_1 \right), \quad (16)$$

$$a_{12} = \frac{imk\alpha_2\Gamma}{b} \frac{K_m(kb)}{K_m(kb) + \alpha_1 K_m'(kb)} \times \left(\frac{K_m(ka)}{I_m(ka)} - \frac{1}{\epsilon_p} \frac{K_m'(ka)}{I_m'(ka)} \right) \times \left(\frac{I_m(kb) - K_m(kb)f_1}{\omega k K_m'(kb) - \alpha_3 K_m(kb)} \right), \quad (17)$$

$$a_{22} = \frac{\omega k^2 \Gamma}{b I_m^2(ka)} \left(\frac{I_m(kb) - K_m(kb)f_1}{\omega k K_m'(kb) - \alpha_3 K_m(kb)} \right), \quad (18)$$

$$b_{11} = \frac{\omega \mu_0 \epsilon_0 \epsilon_p k a \alpha_4 I_m(kb)}{K_m(kb) + \alpha_1 K_m'(kb)} \times \left(\frac{I_m'(ka) K_m(ka)}{I_m^2(ka)} - \frac{1}{\epsilon_p} \frac{K_m'(ka)}{I_m'(ka)} \right), \quad (19)$$

$$b_{12} = \frac{imk\Gamma\alpha_2}{b} \frac{K_m^2(kb)}{f_2} b_{11} - \frac{\Gamma K_m(kb)}{I_m(kb)} \frac{\omega k I_m'(kb) - \alpha_3 I_m(kb)}{\omega k K_m'(kb) - \alpha_3 K_m(kb)} b_{11}, \quad (20)$$

$$b_{22} = \frac{\Gamma}{ka I_m(ka) I_m'(ka)} \frac{imk\alpha_2 I_m(kb) K_m(kb)}{b f_2} - \frac{\Gamma}{ka I_m(ka) I_m'(ka)} \frac{\omega k I_m'(kb) - \alpha_3 I_m(kb)}{\omega k K_m'(kb) - \alpha_3 K_m(kb)}, \quad (21)$$

$$f_1 = \frac{I_m(kb) + \alpha_1 I_m'(kb)}{K_m(kb) + \alpha_1 K_m'(kb)} \quad (22)$$

$$f_2 = (\omega k K_m'(kb) - \alpha_3 K_m(kb))(K_m(kb) + \alpha_1 K_m'(kb)) \quad (23)$$

$$\Gamma = \left(1 - \frac{imk\alpha_2}{b} \frac{K_m^2(kb)}{f_2} \right)^{-1} \quad (24)$$

$$\alpha_1 = \frac{i\omega\epsilon_0 Z_s}{k}, \quad \alpha_2 = \frac{mZ_s}{\mu_0 kb}, \quad \alpha_3 = \frac{iZ_s k^2}{\mu_0}, \quad \alpha_5 = \frac{-iaZ_s}{\mu_0 k^2 b}, \quad (25)$$

In order to validate the general dispersion relation (12), we take the following approximations: First, for a good conducting wall; $Z_s \neq 0$, and for the axially symmetric TM mode; $m=0, \alpha_2=0$. Substituting in (12), we obtain the same result as in [Daqa et al., 2008],

$$\epsilon_p = \frac{\tau_p I_0(\tau_p a)}{\tau_v I_1(\tau_p a)} \frac{I_1(\tau_v a) F + K_1(\tau_v a) G}{I_0(\tau_v a) F - K_0(\tau_v a) G}, \quad (26)$$

where,

$$F = K_0(\tau_v b) - \alpha_1 K_1(\tau_v b),$$

$$G = I_0(\tau_v b) + \alpha_1 I_1(\tau_v b).$$

Second, for a perfect conducting wall; $Z_s=0, \alpha_{1-4}=0$, then (12) becomes,

$$\left(\frac{1}{\tau_p} \frac{I_m'(\tau_p a)}{I_m(\tau_p a)} - \frac{1}{\tau_v} \frac{I_m'(\tau_v a) K_m'(\tau_v b) - I_m'(\tau_v b) K_m'(\tau_v a)}{I_m(\tau_v a) K_m'(\tau_v b) - I_m(\tau_v b) K_m'(\tau_v a)} \right) \times \left(\frac{\epsilon_p I_m'(\tau_p a)}{\tau_p I_m(\tau_p a)} - \frac{1}{\tau_v} \frac{I_m'(\tau_v a) K_m(\tau_v b) - I_m(\tau_v b) K_m'(\tau_v a)}{I_m(\tau_v a) K_m(\tau_v b) - I_m(\tau_v b) K_m(\tau_v a)} \right) = \frac{m^2 k^2}{\omega^2 \mu_0 \epsilon_0 a^2} \left(\frac{\tau_v^2 - \tau_p^2}{\tau_v^2 \tau_p^2} \right)^2 \quad (27)$$

Let $b \rightarrow \infty$; getting the case of a plasma column in vacuum, then (27) reduces to the same result of the study by Akao et al. (Akao & Ida, 1964),

$$\left(\frac{1}{\tau_p} \frac{I_m'(\tau_p a)}{I_m(\tau_p a)} - \frac{1}{\tau_v} \frac{K_m'(\tau_v a)}{K_m(\tau_v a)} \right) \left(\frac{\epsilon_p I_m'(\tau_p a)}{\tau_p I_m(\tau_p a)} - \frac{1}{\tau_v} \frac{K_m'(\tau_v a)}{K_m(\tau_v a)} \right) = \frac{m^2 k^2}{\omega^2 \mu_0 \epsilon_0 a^2} \left(\frac{\tau_v^2 - \tau_p^2}{\tau_v^2 \tau_p^2} \right)^2 \quad (28)$$

Third, applying the quasi-static approximation on (27) (or alternatively substitute $Z_s=0, \alpha_{1-4}=0$, to (15)), we obtain a similar relation that was derived by Trivelpiece (Trivelpiece, 1958),

$$\epsilon_p = \frac{I_m(ka)}{I_m'(ka)} \left(\frac{I_m'(ka) K_m(kb) - I_m(kb) K_m'(ka)}{I_m(ka) K_m(kb) - I_m(kb) K_m(ka)} \right) \quad (29)$$

1.2. Numerical study

In this section we investigate numerically the dispersion relation (15) solely for the dipolar mode; $m=1$. Results are presented in non-dimensional form $\tilde{\omega} = \omega/\omega_p$ vs $\tilde{k} = ka$ to separate geometric effect from absolute size and density. Physical values follow from $\omega = \tilde{\omega} \omega_p$ and $k = \tilde{k}/a$. Hence, for $\omega_p = 1 \times 10^{11}$ rad/s and $a = 0.05$ m the normalized point ($\tilde{\omega} = 0.7, \tilde{k} = 2$) corresponds to $f \approx 11.1$ GHz and $\lambda \approx 0.157$ m.

Part 1: The effect of the ratio of resistive metallic wall radius to plasma radius on the dispersion relation

To design and optimize plasma waveguides, it's crucial to study the effect of changing the radius of plasma column in relation to the metallic pipe's radius. We studied the impact of this parameter by choosing three different ratios; $b/a = 1.5, 2.0, 7.0$, while keeping the wall conductivity of the pipe fixed on the value of stain-steel, i. e., $\sigma = 1.1 \times 10^6$ S/m. The results are plotted in figures 2 and 3. In figure 2, we plot the real part of the normalized frequency ω/ω_p versus the dimensionless quantity ka .

For small values of ka , the increase of the ratio b/a will increase the frequency cutoff value, until the modification of the wall presence diminishes and this can be seen from the green curve that follows the similar behavior of a plasma column in free space in agreement with the finding of Trivelpiece's work (Trivelpiece, 1958) page 59.

Whereas, for large values of ka , all curve go asymptotically to the quasi-static limit for plasma-air boundary, i. e. $\omega/\omega_p=1/\sqrt{2}$. The imaginary part of the normalized frequency ω/ω_p versus the dimensionless quantity ka is plotted in figure 3. For small values of ka , the effect of increasing the ratio b/a ; reducing the impact of the resistive wall presence, introduce a drop and a slight shift to the curves's peaks.

Part 2: The effect of metallic wall conductivity on the dispersion relation

The finite conductivity of the metallic wall leads to electromagnetic energy dissipation in the wall, causes wave damping through Ohmic losses. To study numerically the effect of wall conductivity on the dispersion relation, we swept wall's conductivity over three different values, namely, $\sigma=1\times 10^5, 1\times 10^6, 1\times 10^7$ S/m. whereas the ratio $b/a=2$ is kept constant and the results are plotted in figures 4 and 5. The real part of the normalized frequency ω/ω_p is plotted versus ka , see figure 4. For small values of ka , by decreasing the conductivity, the frequency cutoff increase. For large values of ka , all curve go asymptotically to the quasi-static limit for plasma-air boundary, i. e. $\omega/\omega_p=1/\sqrt{2}$. The resistivity of the pipe's wall introduces an imaginary part to the dispersion relation of the SPW, as shown in figure 5. We see that all curves have almost the same maximum frequency. For small values of ka , by decreasing the wall's conductivity, the full-width half maximum increase, and the maximum frequency is shifted toward higher values of ka .

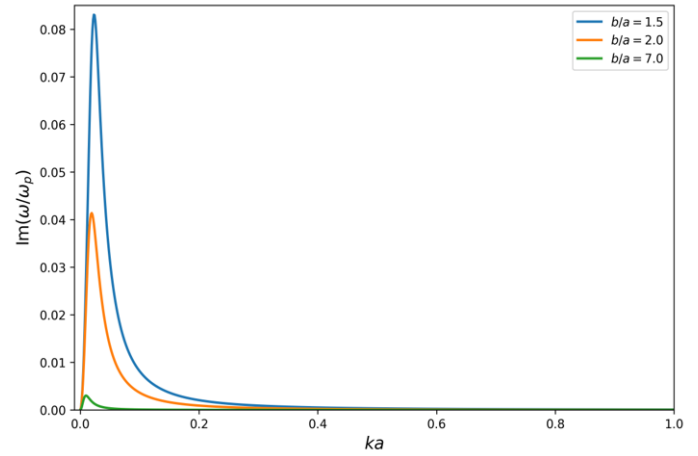


Fig. 3 The imaginary part of the normalized frequency ω/ω_p is plotted versus ka for different values of the ratio of metallic pipe radius to plasma radius b/a . The pipe's conductivity is fixed on the same value as in figure 2.

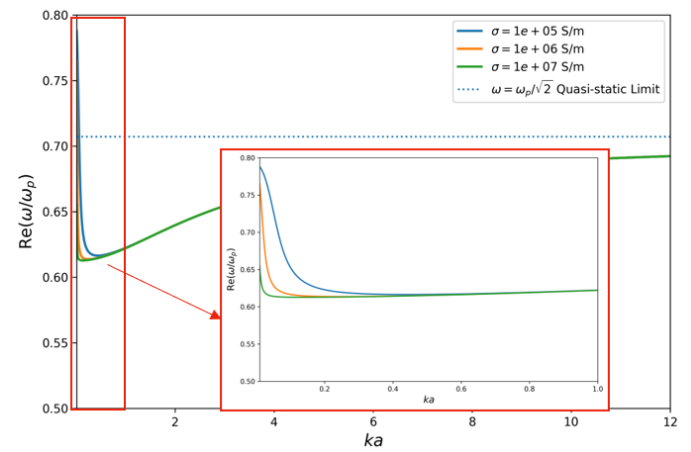


Fig. 4 The real part of the normalized frequency ω/ω_p is plotted versus ka for different values of the metallic pipe conductivity. The pipe is assumed to have the ratio $b/a=2$.

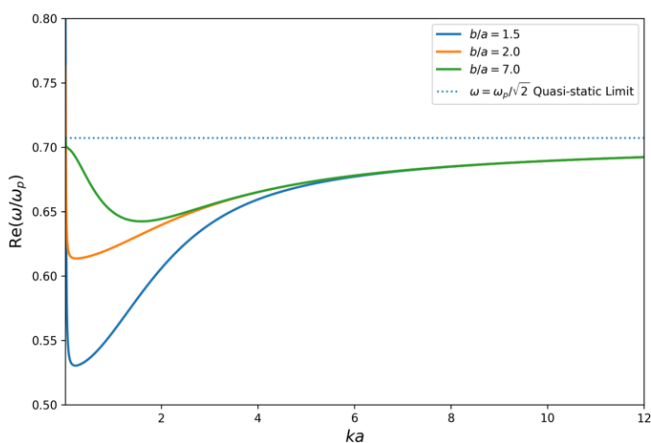


Fig. 2 The real part of the normalized frequency ω/ω_p is plotted versus the dimensionless quantity ka for different values of the ratio of metallic pipe radius to plasma radius b/a . The pipe is assumed to have the conductivity of stain-steel;

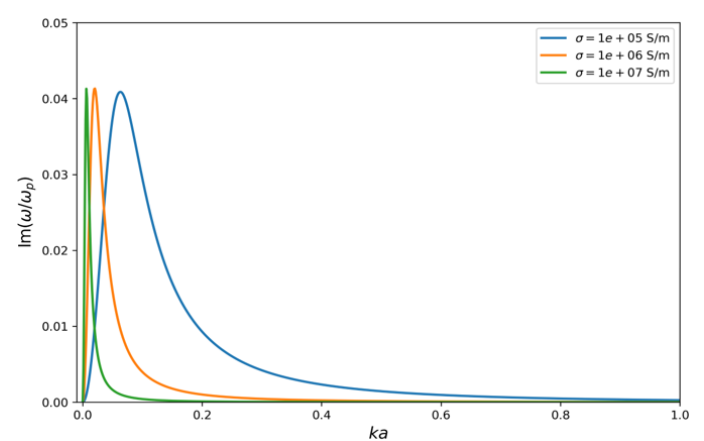


Fig. 5 The imaginary part of the normalized frequency ω/ω_p is plotted versus ka for different values of the metallic pipe conductivity. The pipe's radius is fixed on the same value as in figure 4.

2. CONCLUSION

In this study, we examined a cold, unmagnetized plasma column that partially fills a cylindrical resistive metallic waveguide and is concentric with it. For each azimuthal harmonic number and all surface plasma modes, we analytically developed a general dispersion relation. Next, assuming that the electrostatic approximation is valid, we concentrate the numerical analysis on the dipole mode. The dipole mode, $m=1$, of a partially filled waveguide is identified by all of the obtained results. For a large ka , the real part of the dispersion curves asymptotically increases just below the quasi-static limit, $\omega/\omega_p=1/\sqrt{2}$, which is consistent with the behavior of a surface charge dominated wave. Examining the impact of geometric confinement, the ratio of metallic pipe radius to plasma radius b/a , taking into account the pipe's finite conductivity, reveals that for smaller b/a and from small to mid values of ka , the real part of the dispersion curves begins from positive nonzero values but falls below the quasi-static limit, reaching a profound minimum as we decrease that ratio. For tighter pipes, that is, when the ratio b/a lowers, the cut-off frequency drops. The impact of wall coupling is diminished by greater b/a values. The wall's resistivity, which decreases as the ratio b/a increases, is the cause of the imaginary part of the dispersion relation.

The impact of finite wall conductivity is the subject of the numerical study's second section. Analyzing the dispersion relation's real part reveals that the curve shifts downward and approaches the behavior of a perfect conductor as the conductivity σ increases. In the meantime, the full-width half maximum rises with decreasing conductivity, and the imaginary component of the dispersion relation indicates wall loss that peaks at tiny ka . Additionally, in accordance with skin depth damping, the peak site moves to higher values of ka . The perfect conductor behavior is maintained by taking the infinite conductivity limit. Additionally, we recover the plasma column in the air scenario by assuming that the metal wall radius rises to infinity.

A plasma waveguide system should be designed properly by operating it at a moderate ka and selecting metallic walls with larger b/a and higher conductivity.

Acknowledgements

The author would like to thank Professor A. Alkateeb from Yarmouk University for the significant discussion.

REFERENCES

- A. Al-Khateeb, R. W. Hasse, O. Boine-Frankenheim, and I. Hofmann, "Screening of the resistive-wall impedance by a cylindrical electron plasma," *New J. Phys.*, vol. 10, no. 083008, 2008
- A. Kumar, S.P. Mishra, A. Kumar and A. Varma, "Electron Bernstein wave aided cosh-Gaussian laser beam absorption in plasma," *Optik*, vol. 273, p. 170436, Feb. 2023
- A. Varma, S.P. Mishra, Arvind Kumar and Asheel Kumar, "Laguerre-Gaussian Laser Beam Second Harmonic Generation in Arrays of Vertically Aligned Carbon Nanotube," *Plasmonics*, vol. 20, no. 1, pp. 305–324, Mar. 2024
- A. Varma, S.P. Mishra, Arvind Kumar and Asheel Kumar, "Nonlinear Absorption of Cosh-Gaussian Laser Beam in Arrays of Vertically Aligned Carbon Nanotube," *Plasmonics*, vol. 19, no. 1, pp. 505–521, Aug. 2023
- A. W. Trivelpiece and R. W. Gould, "Space Charge Waves in Cylindrical Plasma Columns," *J. Appl. Phys.*, vol. 30, no. 11, pp. 1784–1793, Nov. 1959
- A. W. Trivelpiece, "Slow Wave Propagation in Plasma Waveguides," Ph.D. dissertation, Caltech, Pasadena, CA, USA, 1958
- B. Ruan, Q. You, J. Zhu, L. Wu, J. Guo, X. Da, and Y. Xiang, "Fano resonance in double waveguides with graphene for ultra-sensitive biosensor," *Optics Express*, vol. 26, no. 13, pp. 16884–16892, 2018
- B. Zotter and S. Kheifets, "Impedances and wakes in high-energy particle accelerators," World Scientific, 1998
- C. S. Liu, "Electron acceleration by surface plasma waves in double metal surface structure," *J. Appl. Phys.*, vol. 102, no. 11, 2007
- Grewal, Gurvikram, and George W. Hanson, "Optically-controlled solid-state plasma leaky-wave antenna," *Microwave and Optical Technology Letters*, vol. 39, no. 6, pp. 450–453, Dec. 2003
- J. Chen, F. Gan, Y. Wang, and G. Li, "Plasmonic sensing and modulation based on Fano resonances," *Adv. Optical Mater.*, vol. 6, no. 9, p. 1701152, Mar. 2018
- L. D. Landau and E. M. Lifshitz, "Electrodynamics of Continuous Media," Pergamon Press, Oxford, 1960
- M. A. Leontovich, "Investigation of radio waves propagation," II issue (Soviet Union Academy of Sciences Publishing House, Russia), 1948
- M. Moisan and Z. Zakrzewski, "Plasma sources based on the propagation of electromagnetic surface waves", *J. Phys. D: Appl. Phys.*, vol. 24, no. 7, pp. 1025-1048, Jan. 1991
- M. Moisan, A. Shivarova and A. W. Trivelpiece, "Experimental investigations of the propagation of surface waves along a plasma column," *Plasma Physics*, vol. 24, no. 11, pp. 1331-1400, Feb. 1982
- Polo Jr, John A., and Akhlesh Lakhtakia, "Surface electromagnetic waves: a review", *Laser & Photonics Reviews*, vol. 5, no. 2, pp. 234-246, Feb. 2011
- S. Sital and E. Sharma, "Surface plasmon modes of dielectric-metal-dielectric waveguides and applications," *IOSR-JECE*, vol. 12, no. 2, pp. 08–19, Apr. 2017
- W. M. Daqa, A. M. Al-Khateeb, A. I. Al-Sharif and N. M. Laham, "Spectra of electromagnetic surface waves on plasma-vacuum interface inside a metallic cylindrical pipe," *Jordan J. Phys.*, vol. 1, no. 1, pp. 9–17, Feb. 2008
- Yasuo Akao and Yoshio Ida, "Electron Density Measurement of a Plasma Column by Surface Wave Resonances," *J. Appl. Phys.*, vol. 35, no. 9, pp. 2565–2570, Sep. 1964
- Yu. M. Aliev, H. Schlüter, and A. Shivarova, "Guided-Wave-Produced Plasmas," Springer, Berlin, 2000